Electronic Supplementary Material (ESI) for ChemComm.

Supporting Information

Self-assembly of a "Cationic-Cage" via formation of Ag-carbene bonds followed by imine condensation

Ritwik Modak,[a] Bijnaneswar Mondal,[a] Prodip Howlader [a] and Partha Sarathi Mukherjee [a]*

[a] *Department of Inorganic and Physical Chemistry, Indian Institute of Science, Bangalore 560012, India. E-mail: psm@iisc.ac.in. Fax: 91-80-2360-1552; Tel; 91-80-2293-3352.*

Table of Contents

EXPERIMENTAL SECTION

Materials and methods: All the chemicals and solvents were purchased from available sources and used without further purification. The NMR spectra were recorded on a Bruker 400 MHz instrument. The chemical shifts (δ) in the ^{1}H, ^{13}C NMR spectra are accounted in ppm relative to TMS (Me_4Si) as an internal standard (0.0 ppm) in $CDCl_3$ or proton resonance resulting from incomplete deuteration of the solvents. High resolution mass spectra were recorded on a Q-TOF instrument by electrospray ionization (ESI) technique using standard spectroscopic grade solvents.

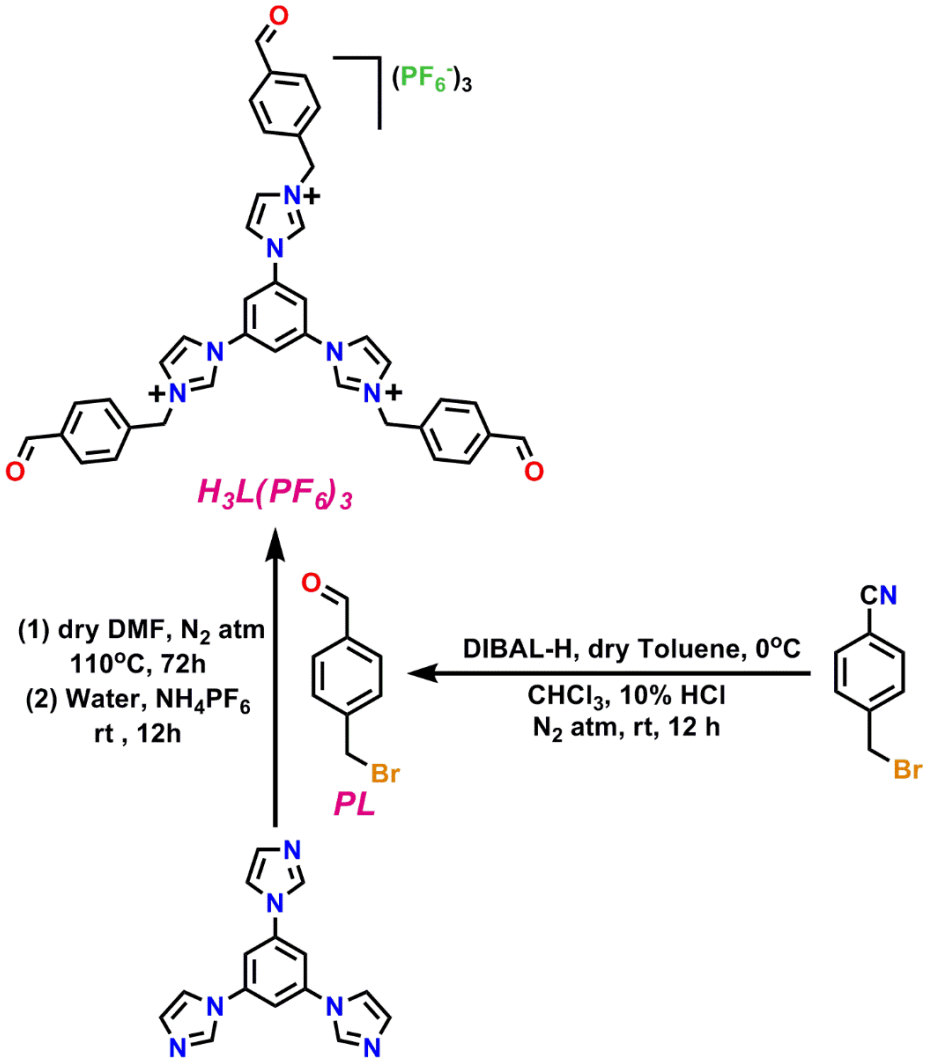

Scheme S1 Synthetic Routes for the preparation of Trialdehyde $H_3\mathbf{L}(PF_6)_3$.

Synthesis of PL: Following a modified procedure from reference[1]: 4-(bromromethyl)benzonitrile (4.00 g, 20.40 mmol) was dissolved in 40 mL dry toluene and cooled to 0°C. 1 M solution of diisobutylaluminumhydride (DIBAL-H) in hexanes (28.8mL) was added dropwise over a period of 2 h under N_2 atmosphere. The resulting mixture was stirred for another hour at 0°C and then diluted with 60 mL of $CHC1_3$. Then, 10% HCl (134 mL) was slowly added and the reaction mixture was stirred at room temperature overnight. The organic layer was washed three times with water, dried over magnesium sulfate, filtered, and evaporated to afford the crude product. Needle-like crystal was obtained by recrystallizing form hexane with isolated yield 86.19% (3.5 g, 17.584 mmol). ^{1}H NMR ($CDCl_3$, 400 MHz) δ 10.00 (s, 1H), 7.85 (d, 2H), 7.55 (d, 2H), 4.51 (s, 2H).

Synthesis of H_3**L**$(PF_6)_3$**:** A solution of 1, 3, 5-tris(1-imidazolyl)benzene (0.83 g, 3.0 mmol) and **PL** (2.0 g, 10.0 mmol) in dry DMF (30 mL) was stirred at 110 ℃ for 72 h under N_2 atmosphere. The resulting precipitate was filtered, washed with acetonitrile and diethyl ether, and dried in vacuo to afford a white solid. This white solid was re-dissolved in 30 mL water and NH_4PF_6 (5.0 g) was then added to the aqueous solution. The white precipitate was collected and washed with water to give the desired trialdehyde H_3**L**$(PF_6)_3$ as a white powder. Isolated Yield: 92.67% (2.97 g, 2.78 mmol). ^{1}H NMR (CD_3CN, 400MHz): δ 10.05 (s, 3H), 9.09 (s, 3H), 8.07 (s, 3H), 8.00 (d, 6H), 7.93 (s, 3H), 7.72 (s, 3H), 7.67 (d, 6H), 5.59 (s, 6H) .^{13}C NMR (100 MHz, CD_3CN): δ 193.1, 139.9, 138.1, 137.9, 136.6, 131.1, 130.5, 125.1, 123.4, 119.8, 54.2. ESI-HRMS (CH_3CN): m/z for $C_{39}H_{33}N_6O_3P_3F_{18}$: $[M\text{-}PF_6]^{1+}$ 923.1774 (calcd 923.1898), $[M\text{-}2PF_6]^{2+}$ 389.1056 (calcd 389.1128).

Synthesis of OC-Ag: The suspension of H_3**L**$(PF_6)_3$ (1.24 g, 1.592 mmol) and Ag_2O (0.553 g, 2.388 mmol) in 10 mL acetonitrile was heated to 60^o C for 24 h under exclusion of light. After cooling to ambient temperature, the resulting suspension was filtered. The filtrate was concentrated to 5 mL, and addition of diethyl ether (30 mL) induced precipitation of a white solid, which was collected by filtration, washed with diethyl ether, and dried in vacuo. Isolated Yield: 70.16% (2.256 g, 1.117 mmol). ^{1}H NMR (CD_3CN, 400MHz): δ 9.93 (s, 6H), 7.73 (d, 12H), 7.59 (s, 6H), 7.50 (d, 6H), 7.44 (d, 6H), 7.32 (d, 12H), 5.38 (s, 12H) .^{13}C NMR (100 MHz, CD_3CN): δ 193.0, 180.7, 143.7, 142.2, 137.3, 130.9, 129.2, 124.8, 123.3, 121.9, 55.4. ESI-HRMS (CH_3CN): m/z for $C_{78}H_{60}N_{12}O_6P_3F_{18}Ag_3$: $[M\text{-}PF_6]^{1+}$ 1875.1267 (calcd 1875.1277), $[M\text{-}2PF_6]^{2+}$ 865.0804 (calcd 865.0784).

Crystals suitable for an X-ray diffraction study were obtained by diffusion of diethyl ether/ethanol into a saturated acetone/acetonitrile solution of **OC-Ag**.

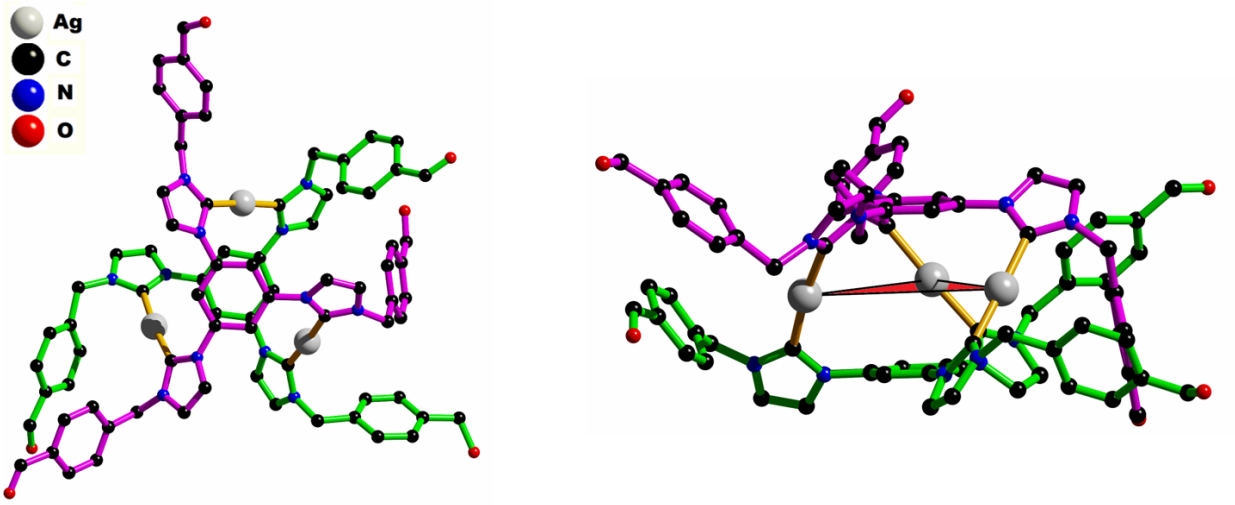

Fig. S1 X-ray crystal structure of **OC-Ag**. Hydrogen atoms are omitted for clarity. Ball-stick model, Top view (left) and Side view (right).

Table S1 Crystallographic Data and Refinement Parameter of **OC-Ag**

	OC-Ag
Formula	$C_{78}\ H_{60}\ Ag_3\ F_{18}\ N_{12}\ O_6\ P_3$
Molecular weight	2018.89
Temperature (K)	100(2)
Crystal system	monoclinic
Space group	P21/c
a (Å)	20.5748(18)
b (Å)	21.1941(18)
c (Å)	19.7887(17)
***α* (°)**	90.00
***β* (°)**	90.633(2)
***γ* (°)**	90.00
***V* (Å^3)**	8628.6(13)
Z	4
ρ_c (g cm^{-3})	1.554
μ (mm^{-1})	0.825
***F*(000)**	4028
Crystal size (mm^3)	0.30 × 0.40 × 0.50
***θ* (°)**	2.817–25.00
Limiting indices	$-24 \le h \le 24$
	$-25 \le k \le 25$

	$-23 \le l \le 23$
No. of reflections collected	222247
No. of independent refl. (R_{int})	15165
Completeness to θ /%	99.8
No. of data/restraints/params	15165/1095/1155
Goodness of fit (GOF) on F^2	1.068
Final *R* indices ($I > 2\,\theta\,(I)$)	
R_1	0.0765[a]
wR_2	0.1780[b]
***R* indices (all data)**	
R_1	0.1259[a]
wR_2	0.1988[b]
Largest difference in peak, hole (e Å^{-3})	1.947, -1.138

[a] $R_1 = \Sigma(|F_o| - |F_c|)/\Sigma|F_o|$. [b] $wR_2 = \{\Sigma[w(|F_o|^2 - |F_c|^2)^2]/\Sigma[w(|F_o|^2)^2]\}^{1/2}$

Synthesis of CC-Ag: In a glass vial, **OC-Ag** (21 mg, 0.01 mmol) was taken in CD_3CN and then 3.1 equivalents of 1,4-diaminobutane (2.84 mg, 0.032 mmol) was slowly added to it. After keeping the glass vial at room temperature for 24h, ^{1}H, 2D NMR and mass spectra of the corresponding solutions were recorded. Same reaction protocol and condition were followed for the DMSO-D_6 solvent. ^{1}H NMR (CD_3CN, 400MHz): δ 8.23 (s, 6H), 7.57 (d, 12H), 7.52 (s, 6H), 7.45 (s, 6H), 7.39 (s, 6H), 7.19 (d, 12H), 5.31 (d, 12H), 3.56-3.58 (m, 12H), 1.62-1.64 (m, 12H). ^{1}H NMR (DMSO-D_6, 400MHz): δ 8.26 (s, 6H), 7.91 (s, 6H), 7.79 (s, 6H), 7.75 (s, 6H), 7.56 (d, 12H), 7.21 (d, 12H), 5.40-5.58 (m, 12H), 3.55-3.58 (m, 12H), 1.61-1.65 (m, 12H).^{13}C NMR (100 MHz, DMSO-D_6): δ 180.1, 153.3, 140.2, 135.7, 134.8, 130.4, 130.1, 126.2, 124.2, 121.5, 55.3, 45.1, 33.2. ESI-HRMS (CH_3CN): m/z for $C_{90}H_{84}N_{18}P_3F_{18}Ag_3$: $[M\text{-}2PF_6]^{2+}$ 943.1987 (calcd 943.1985), $[M\text{-}3PF_6]^{3+}$ 580.4722 (calcd 580.4784).

Synthesis of CC-Au: A solution of Au(THT)Cl (13 mg, 0.04 mmol) in DMSO-D_6 was slowly added to the above-mentioned **CC-Ag** solution (DMSO-D_6) (21 mg, 0.01 mmol) in a glass vial. After stirring for 12h at room temperature, the solution was centrifuged to get a clear solution. ^{1}H, 2D NMR and mass spectra of the corresponding solution was recorded. ^{1}H NMR (DMSO-D_6, 400MHz): δ 8.25 (bs, 6H), 7.94-7.86 (bm, 18H), 7.53 (bs, 12H), 7.24 (bs, 12H), 5.47-5.55 (bd, 12H), 3.55(bs, 12H), 1.62 (bs, 12H).^{13}C NMR (100 MHz, DMSO-D_6): δ 182.6, 153.5, 140.4, 135.9, 135.0, 130.6, 130.3, 126.7, 124.7, 122.4, 55.8, 45.9, 33.3. ESI-HRMS (DMSO-CH_3CN): m/z for $C_{90}H_{84}N_{18}P_3F_{18}Au_3$: $[M\text{-}2PF_6]^{2+}$ 1076.8012 (calcd 1076.7975), $[M\text{-}3PF_6]^{3+}$ 669.5369 (calcd 669.5381).

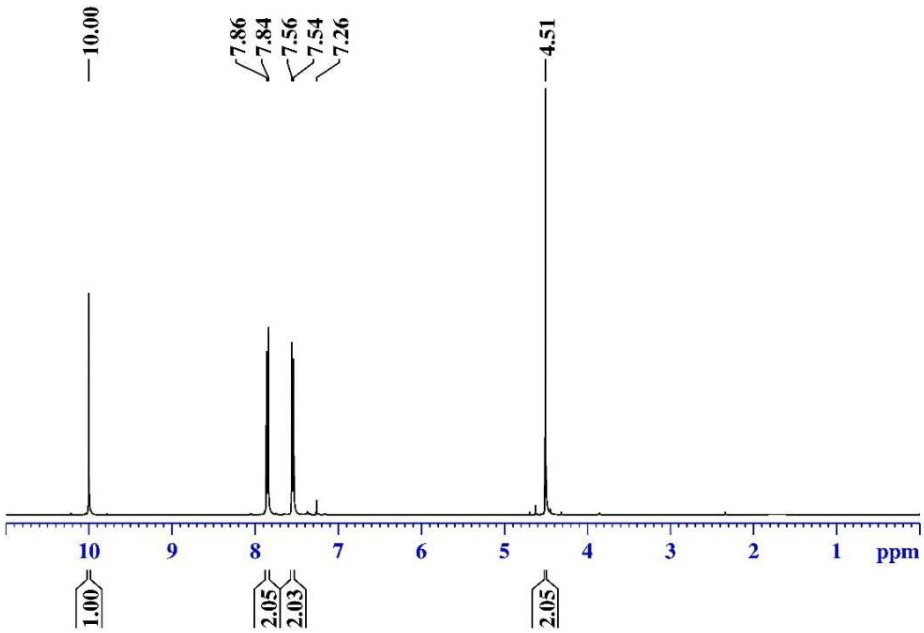

Fig. S2 ^{1}H NMR spectrum of **PL** recorded in $CDCl_3$.

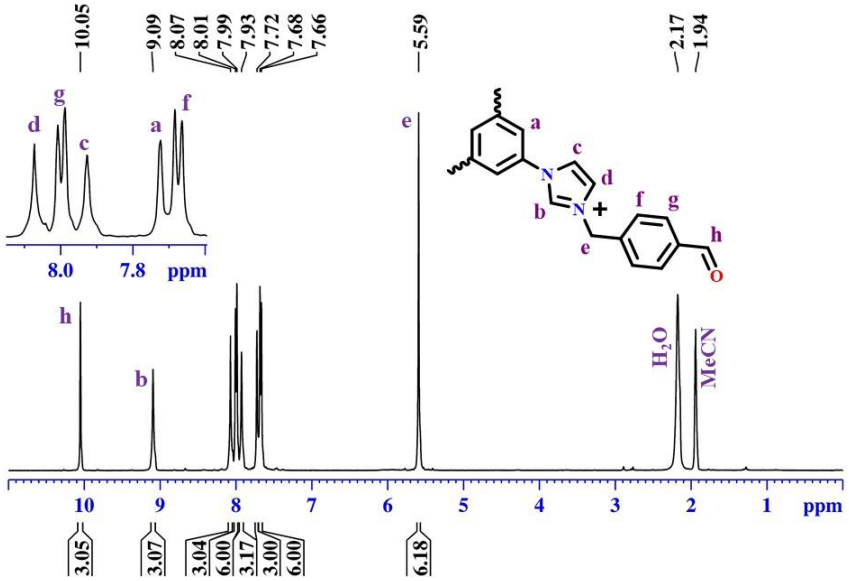

Fig. S3 ^{1}H NMR spectrum of H_3**L** $(PF_6)_3$ recorded in CD_3CN.

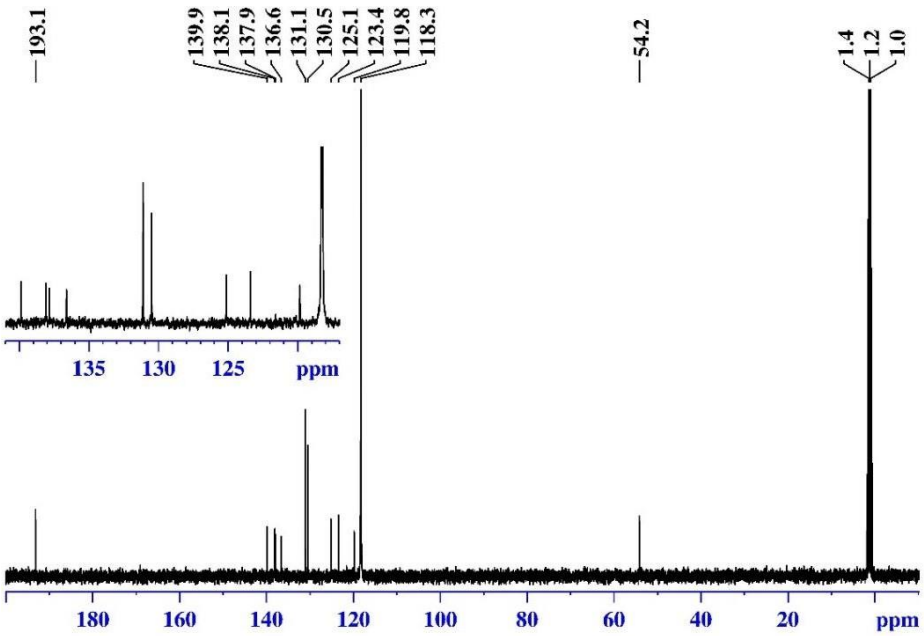

Fig. S4 ^{13}C NMR spectrum of H_3**L** $(PF_6)_3$ recorded in CD_3CN.

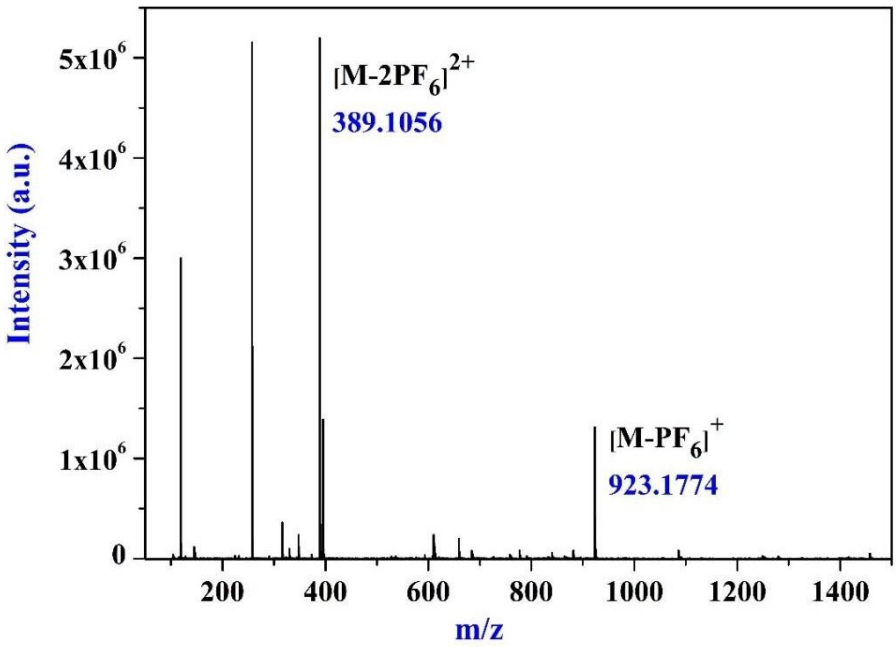

Fig. S5 ESI-HRMS spectrum of cage H_3**L**$(PF_6)_3$ recorded in CH_3CN.

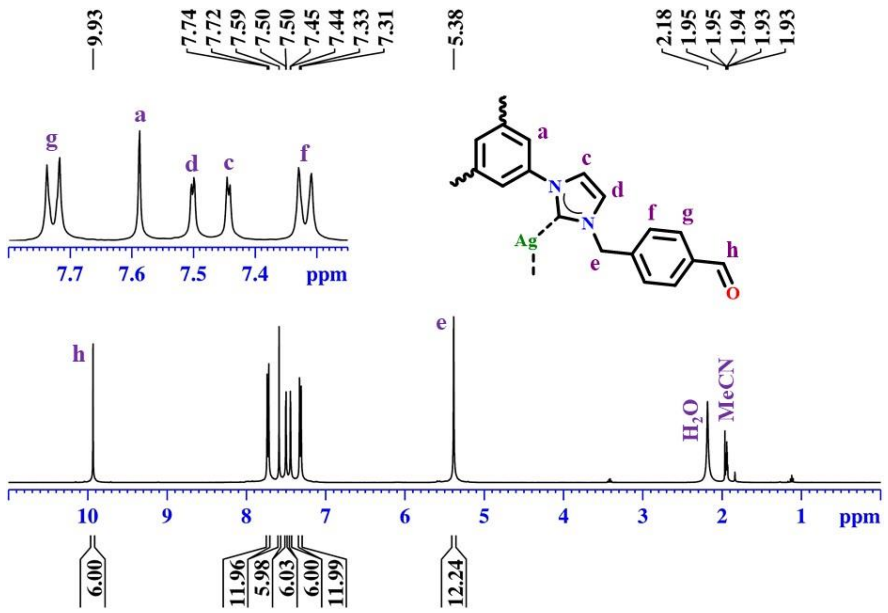

Fig. S6 ^{1}H NMR spectrum of **OC-Ag** recorded in CD_3CN.

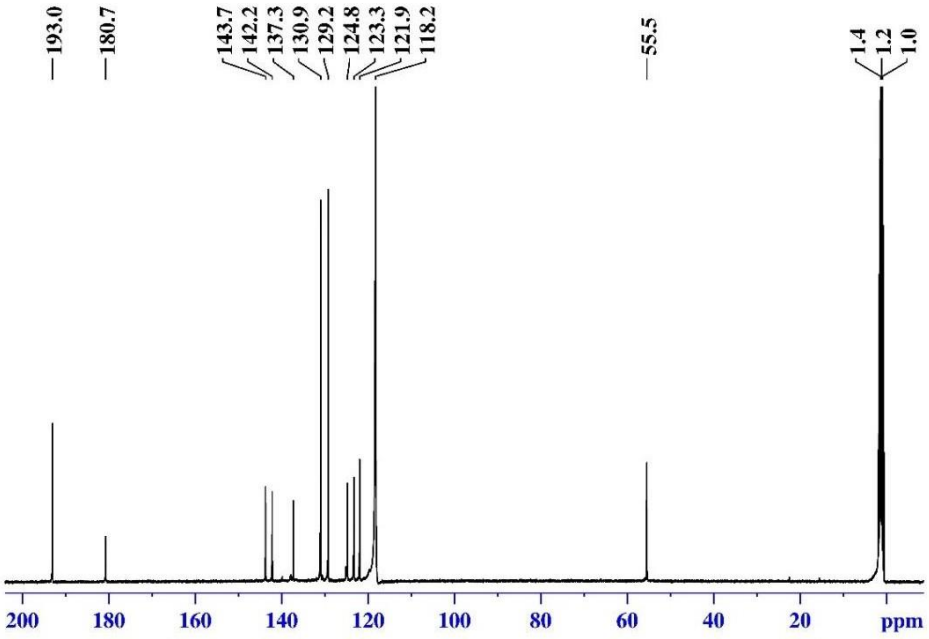

Fig. S7 ^{13}C NMR spectrum of **OC-Ag** recorded in CD_3CN.

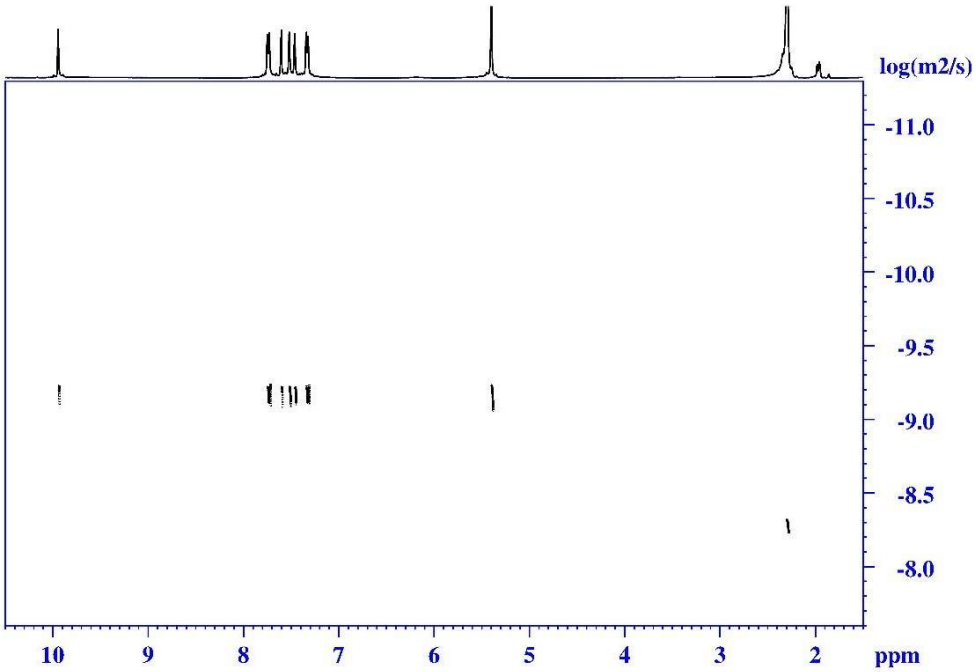

Fig. S8 ^{1}H 2D DOSY NMR spectrum of cage **OC-Ag** recorded in CD_3CN.

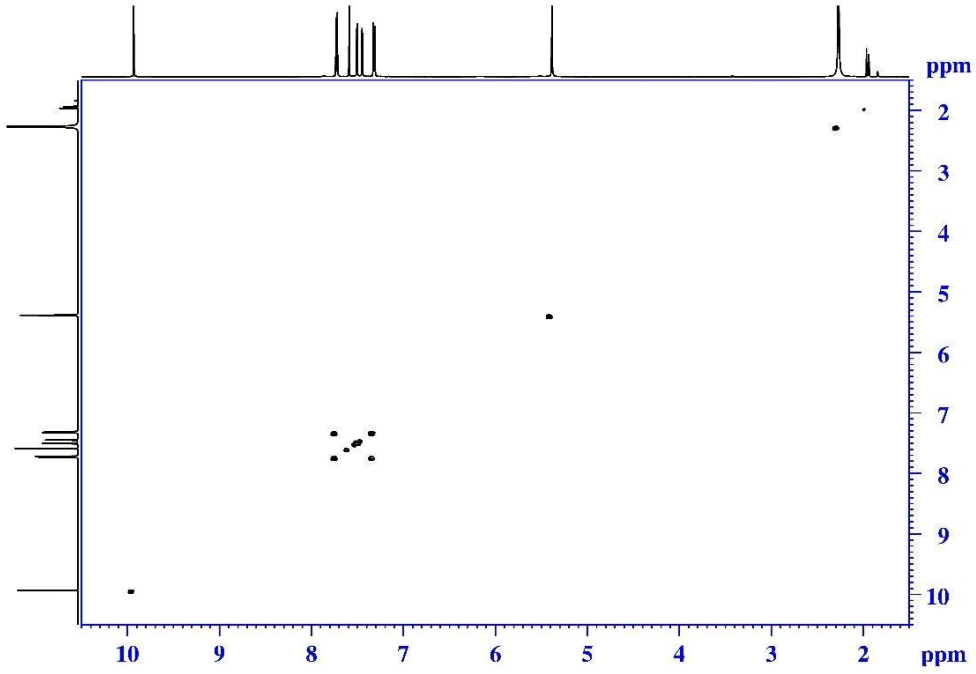

Fig. S9 ^{1}H 2D COSY NMR spectrum of cage **OC-Ag** recorded in CD_3CN

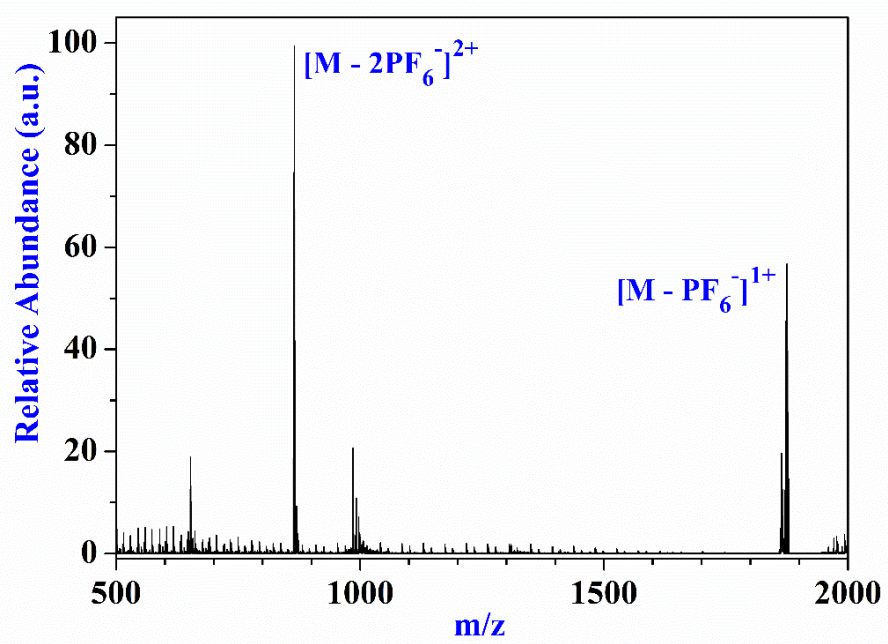

Fig. S10 ESI-HRMS spectrum of cage **OC-Ag** recorded in CH_3CN.

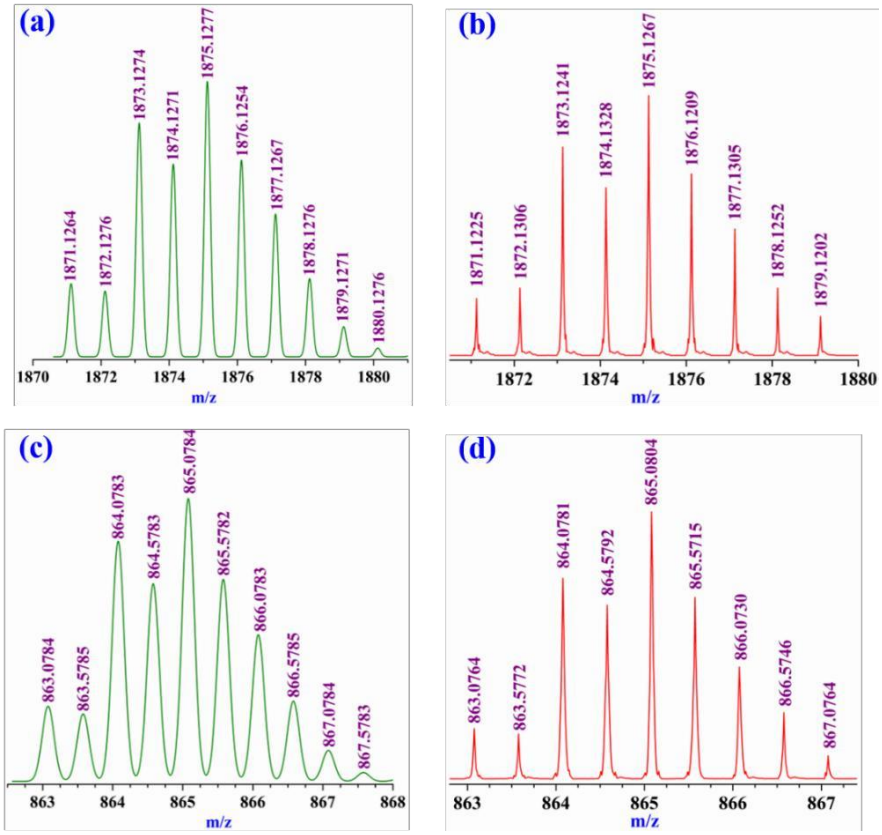

Fig. S11 Theoretical (green) and experimental (red) isotopic patterns of the fragments **[M-PF_6^-]$^{1+}$** (a, b) and **[M-2PF_6^-]$^{2+}$** (c, d) of cage **OC-Ag** recorded in CH_3CN.

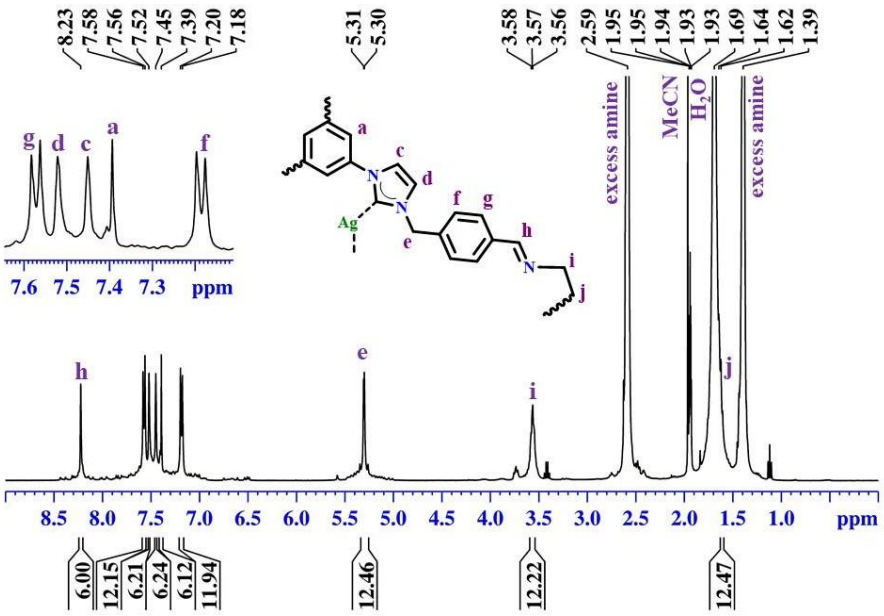

Fig. S12 ^{1}H NMR spectrum of **CC-Ag** recorded in CD_3CN.

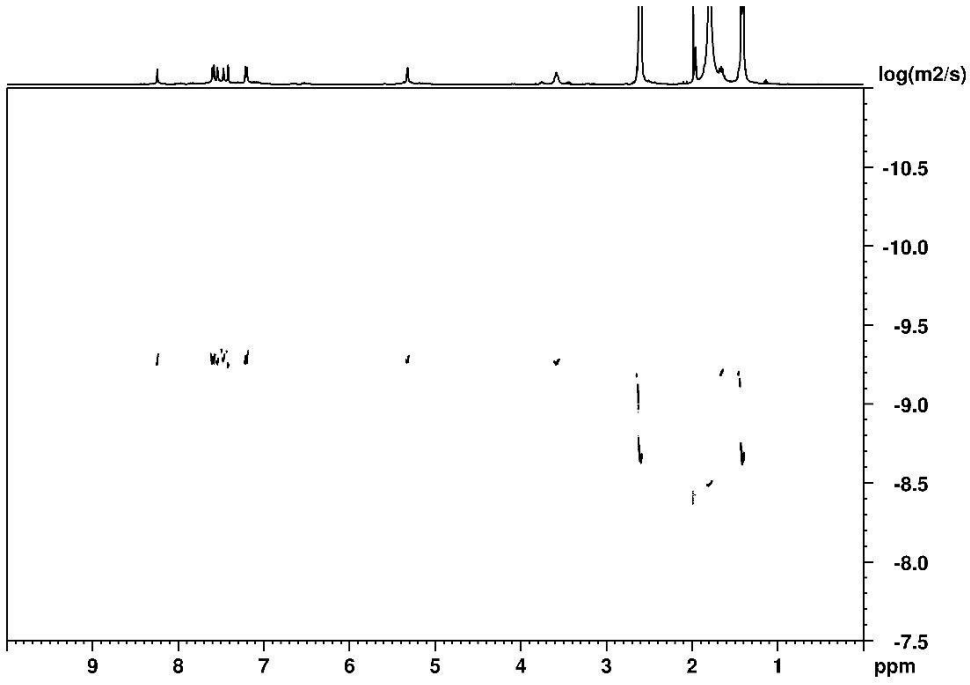

Fig. S13 ^{1}H 2D DOSY NMR spectrum of cage **CC-Ag** recorded in CD_3CN.

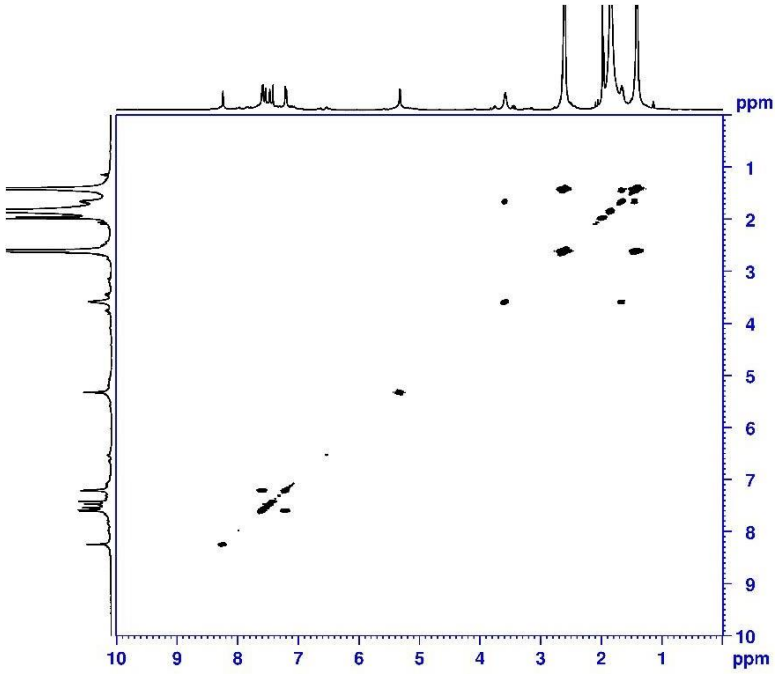

Fig. S14 ^{1}H 2D COSY NMR spectrum of cage **CC-Ag** recorded in CD_3CN.

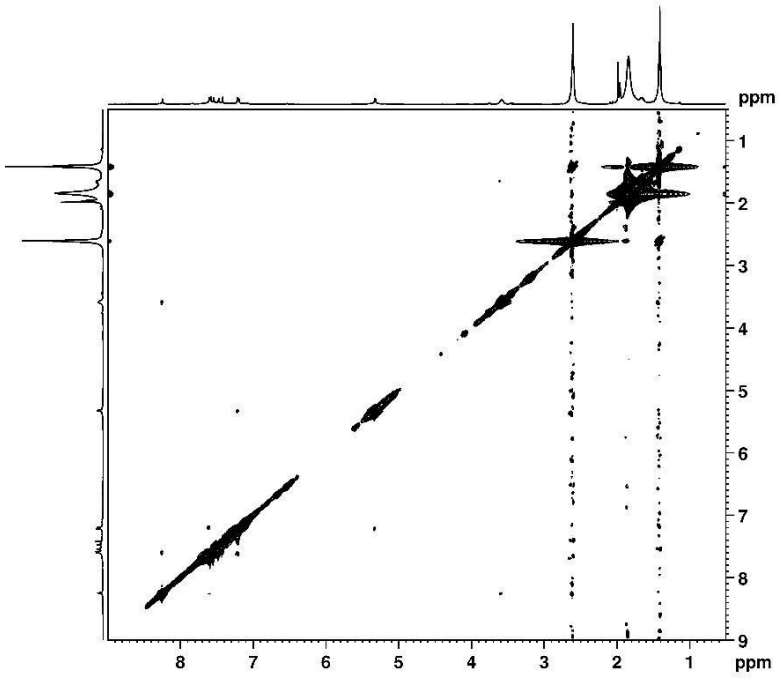

Fig. S15 ^{1}H 2D NOESY NMR spectrum of cage **CC-Ag** recorded in CD_3CN.

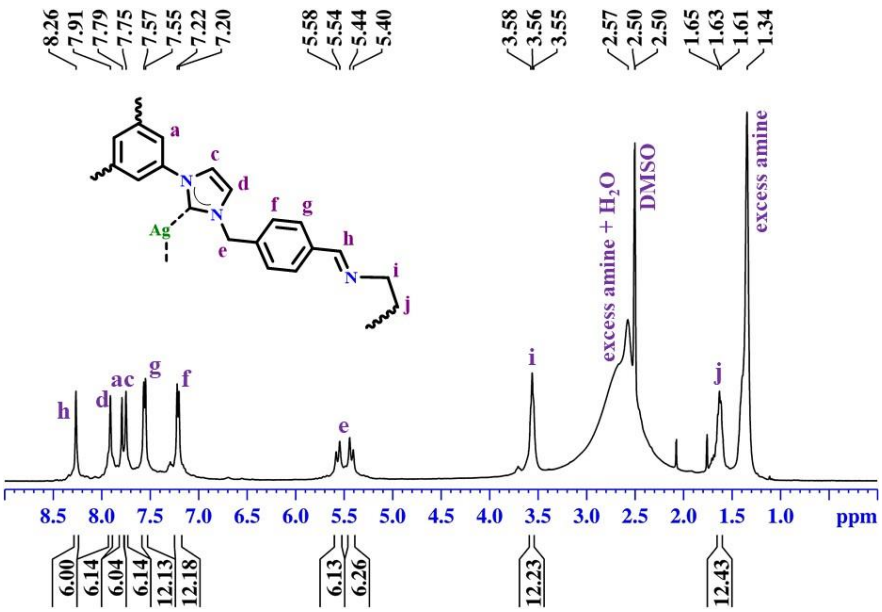

Fig. S16 ^{1}H NMR spectrum of **CC-Ag** recorded in DMSO-D_6.

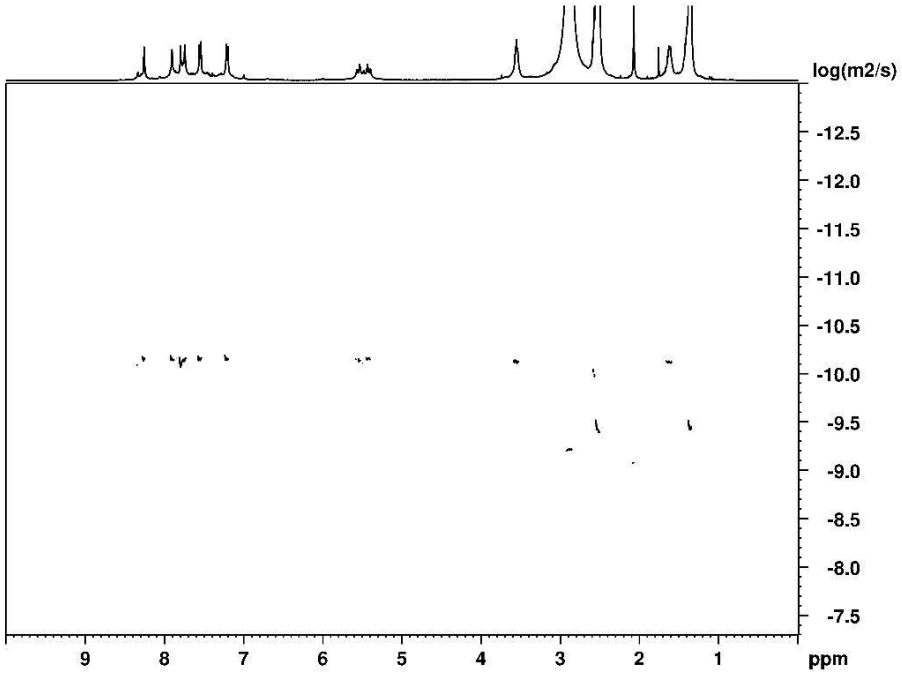

Fig. S17 ^{1}H 2D DOSY NMR spectrum of cage **CC-Ag** recorded in DMSO-D_6.

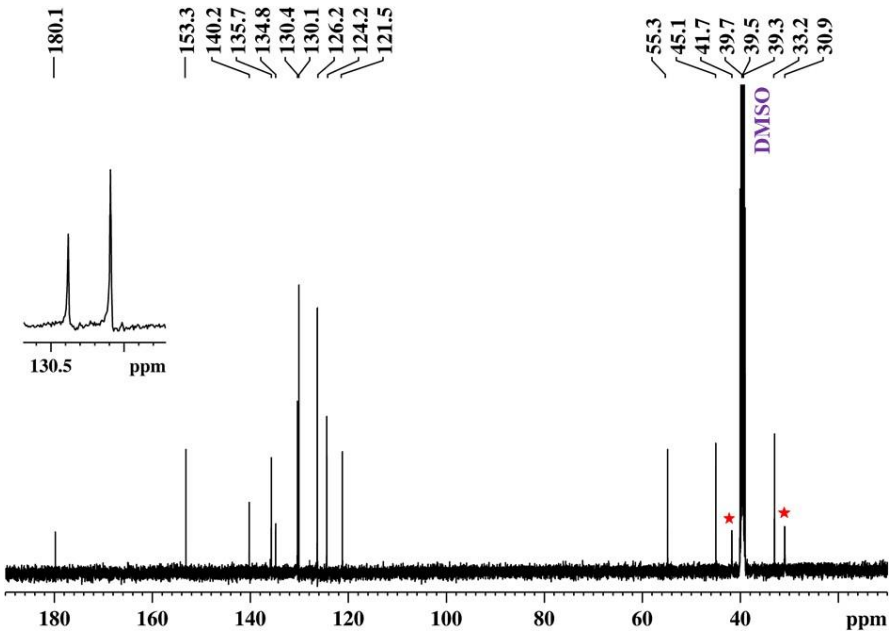

Fig. S18 ^{13}C NMR spectrum of **CC-Ag** recorded in DMSO-D_6. Extra peaks at 41.7 and 30.9 ppm correspond to excess 1, 4-diaminobutane.

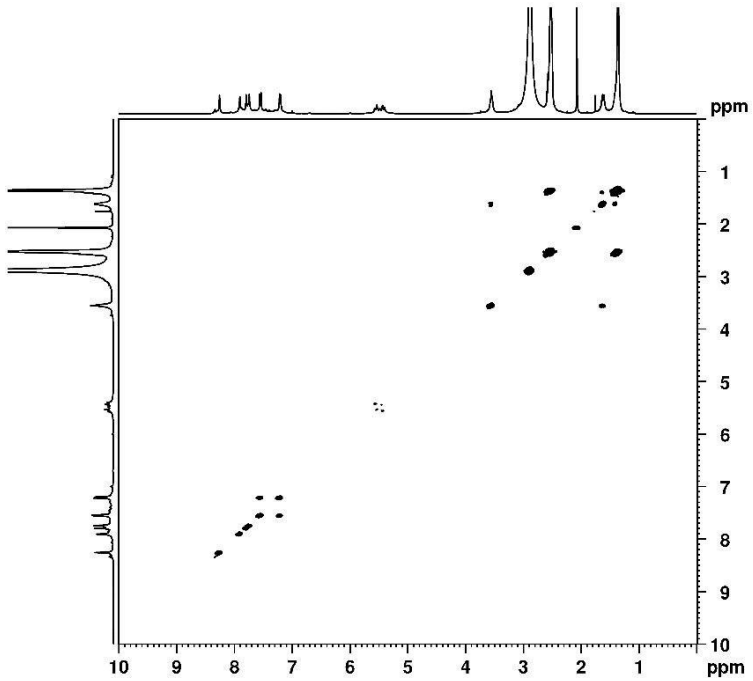

Fig. S19 ^{1}H 2D COSY NMR spectrum of cage **CC-Ag** recorded in DMSO-D_6.

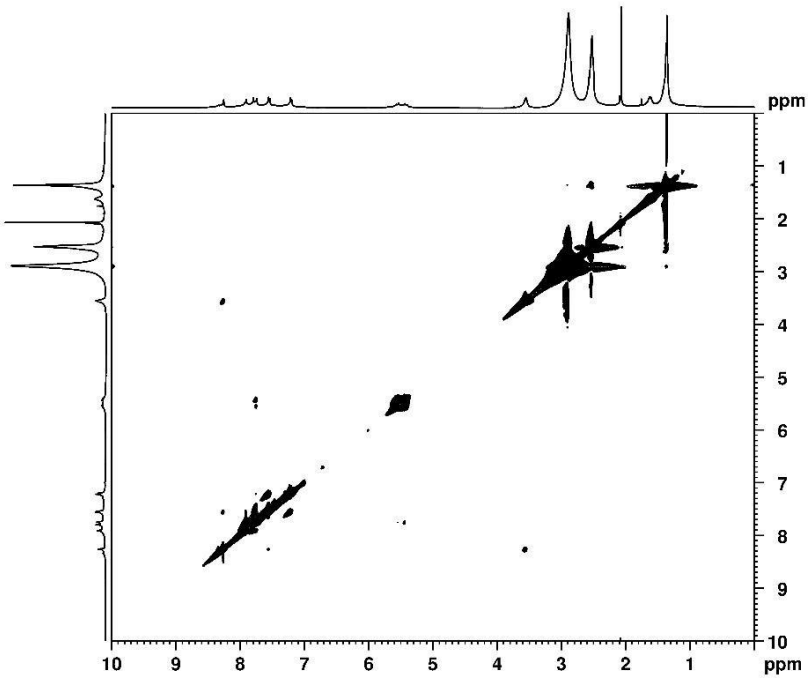

Fig. S20 ^{1}H 2D NOESY NMR spectrum of cage **CC-Ag** recorded in DMSO-D_6.

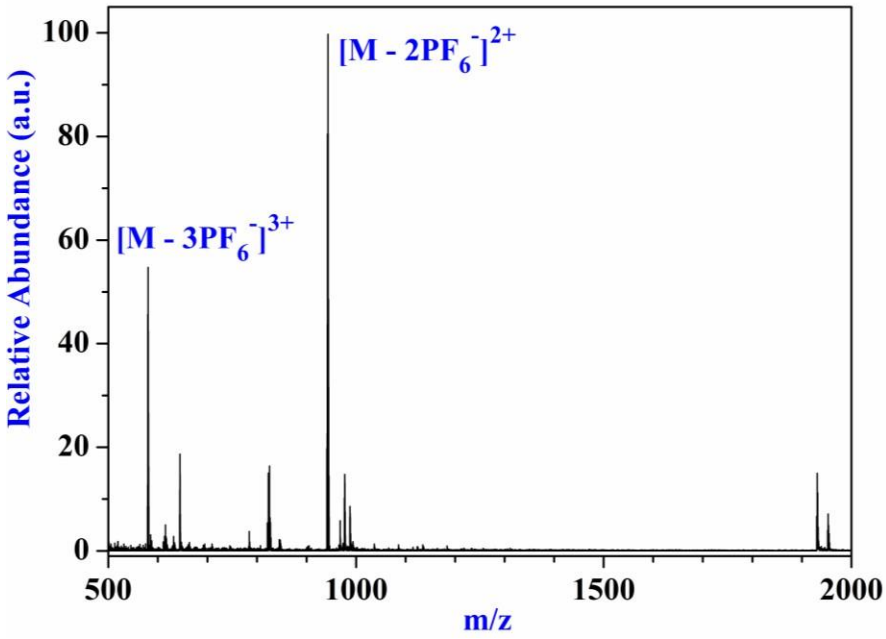

Fig. S21 ESI-HRMS spectrum of cage **CC-Ag** recorded in CH_3CN.

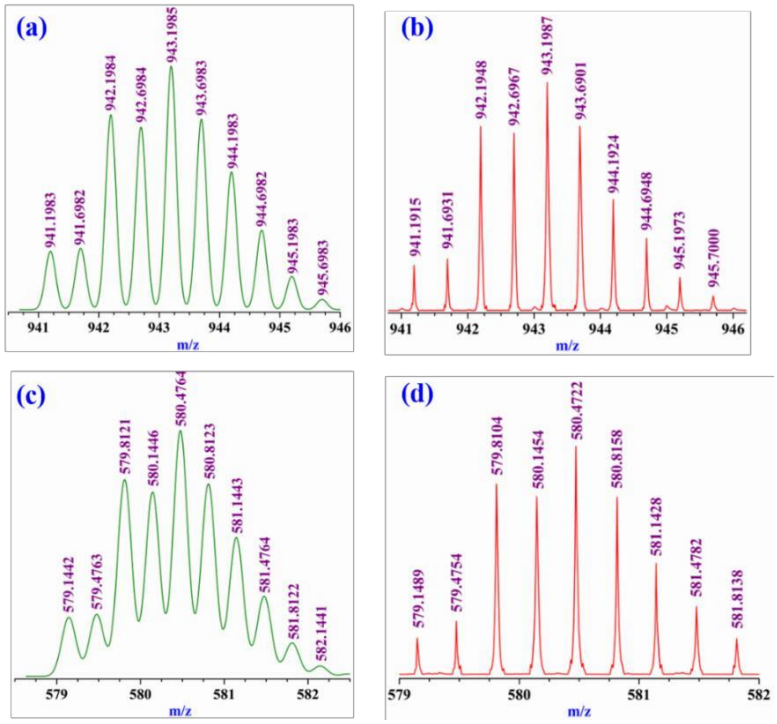

Fig. S22 Theoretical (green) and experimental (red) isotopic patterns of the fragments **[M-2PF$_6^-$]$^{2+}$** (a, b) and **[M-3PF$_6^-$]$^{3+}$** (c, d) of cage **CC-Ag** recorded in CH_3CN.

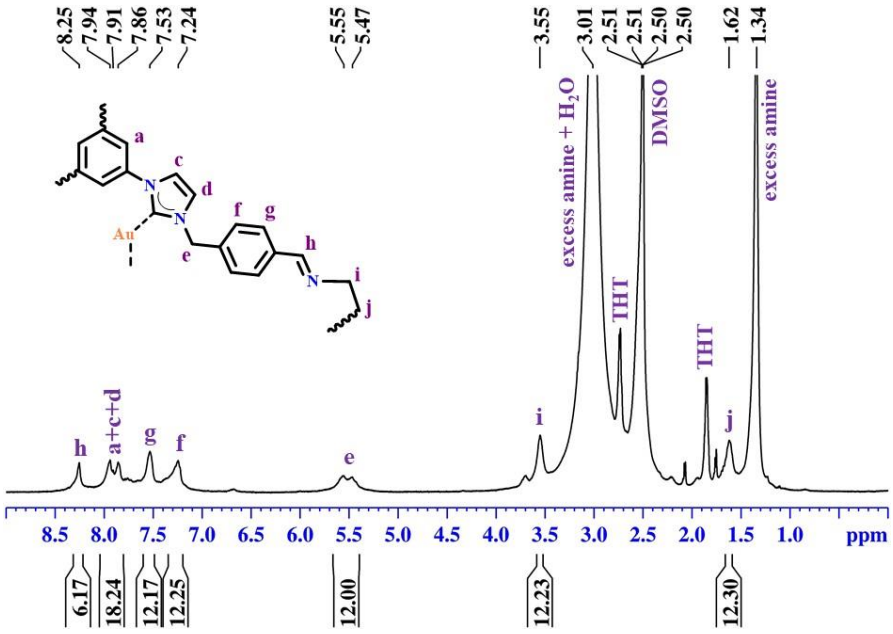

Fig. S23 ^{1}H NMR spectrum of **CC-Au** recorded in DMSO-D_6.

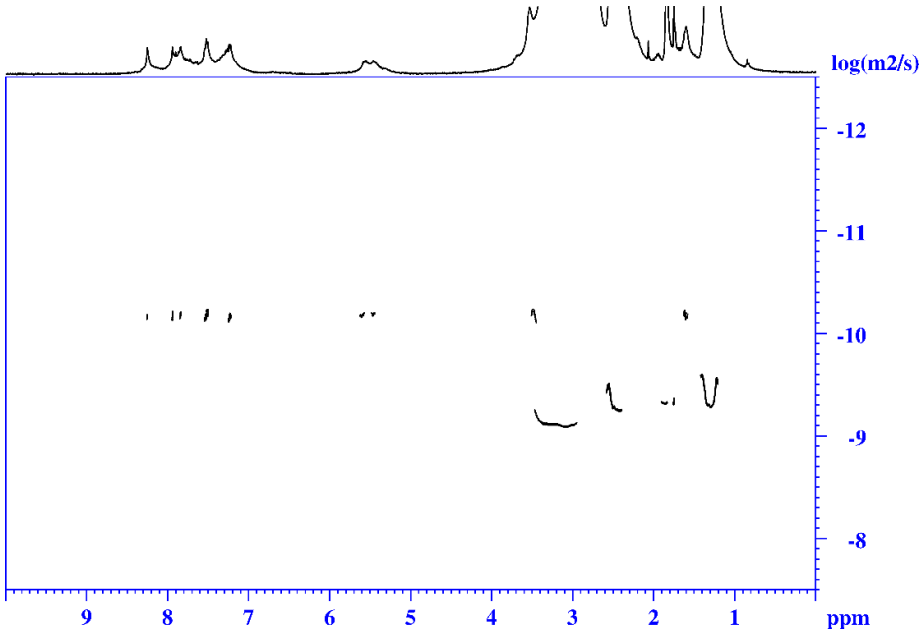

Fig. S24 ^{1}H 2D DOSY NMR spectrum of cage **CC-Au** recorded in DMSO-D_6.

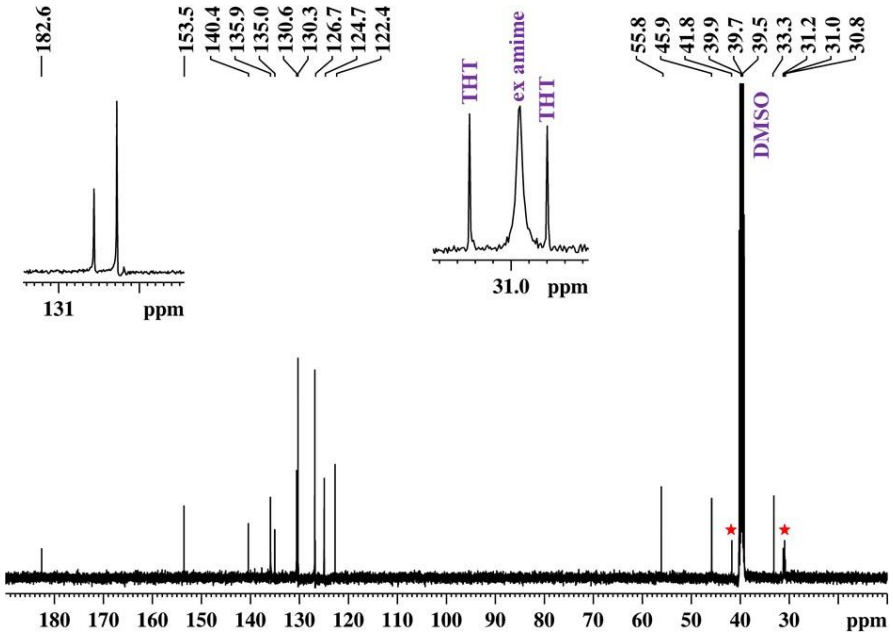

Fig. S25 ^{13}C NMR spectrum of **CC-Au** recorded in DMSO-D_6. Extra peaks at 41.8, 31.0, 30.8 and 31.2 ppm correspond to excess 1, 4-diamino butane and THT.

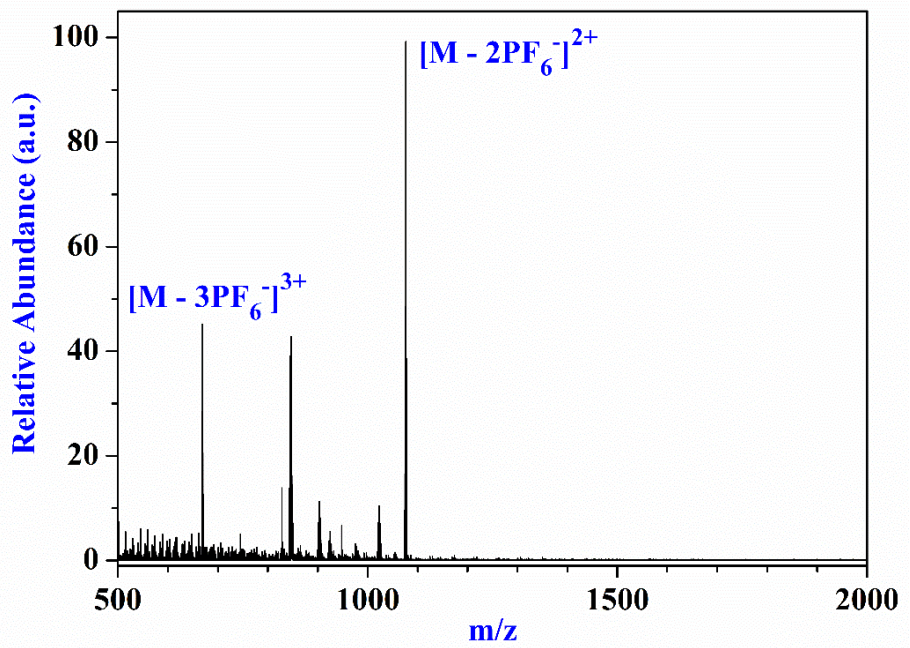

Fig. S26 ESI-HRMS spectrum of cage **CC-Au** recorded in DMSO-CH_3CN.

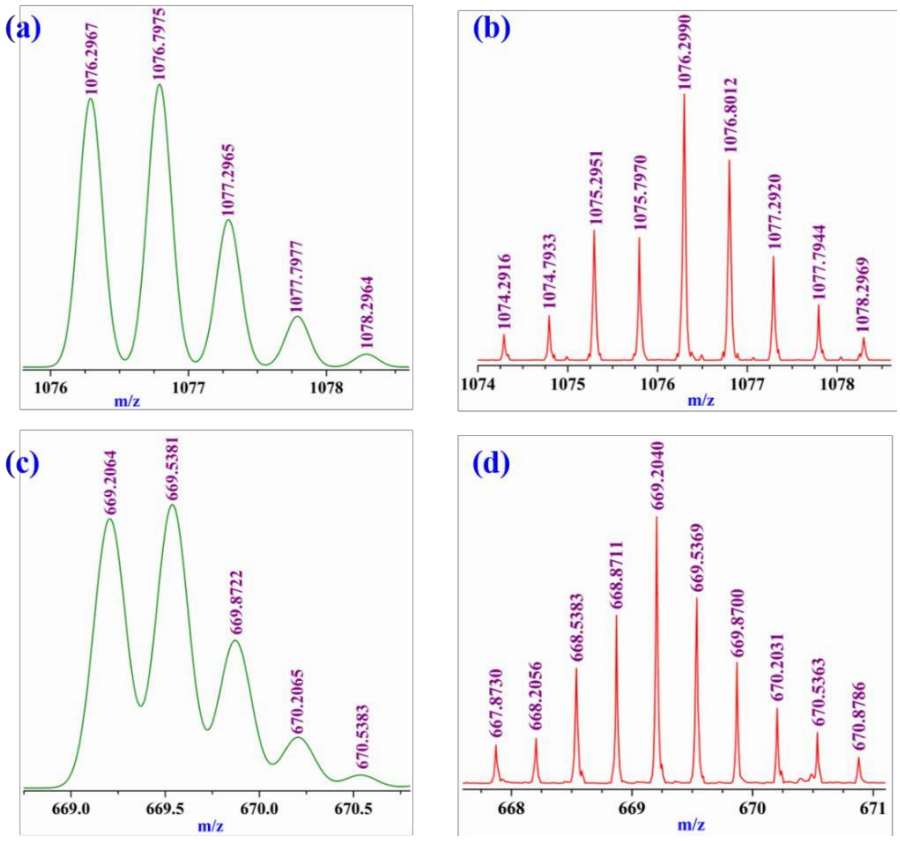

Fig. S27 Theoretical (green) and experimental (red) isotopic patterns of the fragments **[M-2PF_6^-]$^{2+}$** (a, b) and **[M-3PF_6^-]$^{3+}$** (c, d) of cage **CC-Au** recorded in DMSO-CH_3CN.

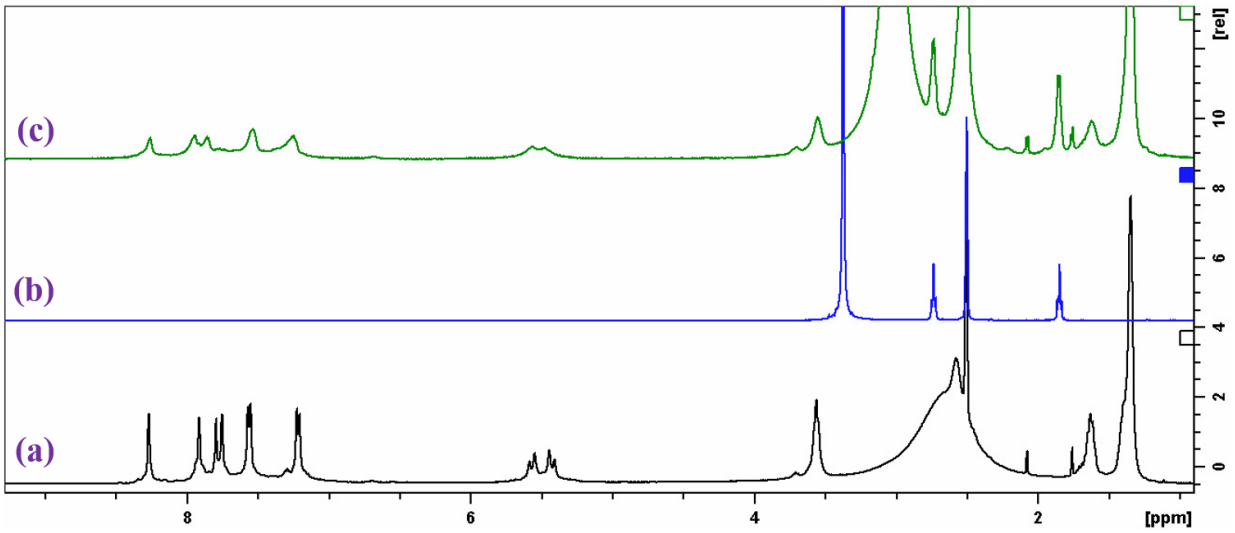

Fig. S28 ^{1}H NMR spectrum comparison of (a) **CC-Ag**, (b) **THT** and (c) **CC-Au** recorded in DMSO-D_6.

Diffusion NMR experiment:

Diffusion ordered spectroscopy (DOSY) NMR was performed on a Bruker 400 MHz NMR spectrometer. The samples of cage **CC-Ag** and **CC-Au** were measured using DMSO-D_6 as the solvent at 298K. The effective hydrodynamic radius R was calculated using the Stokes-Einstein equation: $D = (k_BT)/(6\pi\eta R)$, where D is the diffusion coefficient, k_B is the Boltzmann constant (1.38×10^{-23} $m^2kgs^{-2}K^{-1}$), T is absolute temperature (298K), η is the viscosity of DMSO-D_6 (2.19×10^{-3} $kgm^{-1}s^{-1}$) and MeCN-D_3 (3.9×10^{-4} $kgm^{-1}s^{-1}$) at 298K.

Table S2: Diffusion coefficient and Hydrodynamic radius calculation.

Sample	***Solvent***	***Diffusion coefficient [log(m^2/s)]***	***Calculated radius (nm)***
OC-Ag	MeCN-D_3	-9.19 ± 0.01	0.86 ± 0.02
CC-Ag	DMSO-D_6	-10.16 ± 0.01	1.44 ± 0.03
CC-Au	DMSO-D_6	-10.18 ± 0.01	1.50 ± 0.03

Computational Methodology: Full geometry optimizations were performed using Gaussian 09-d package.[2] Calculations were done using dispersion-corrected DFT-D3 as developed by Grimme [3,4] and a hybrid B3LYP functional was used in all calculations as implemented in Gaussian 09-d package. A mixed basis set (SDD for the Ag and 6-31g for all other atoms) was used for all

calculations. The result indicates that **CC-Ag^{I}** is more energetically favoured assembly than **CC-Ag^{II}** (Table S3).

Table S3: Total energies of **CC-Ag^{I}** and **CC-Ag^{II}**.				
Assembly	Method	Basis set	Total Energy (a.u.)	Total Energy (Kcal/mol)
CC-Ag^{I}	DFT/B3LYP-D3	SDD/6-31g	-4905.76881449	-3078369.9310
CC-Ag^{II}	DFT/B3LYP-D3	SDD/6-31g	-4905.73424433	-3078348.2383

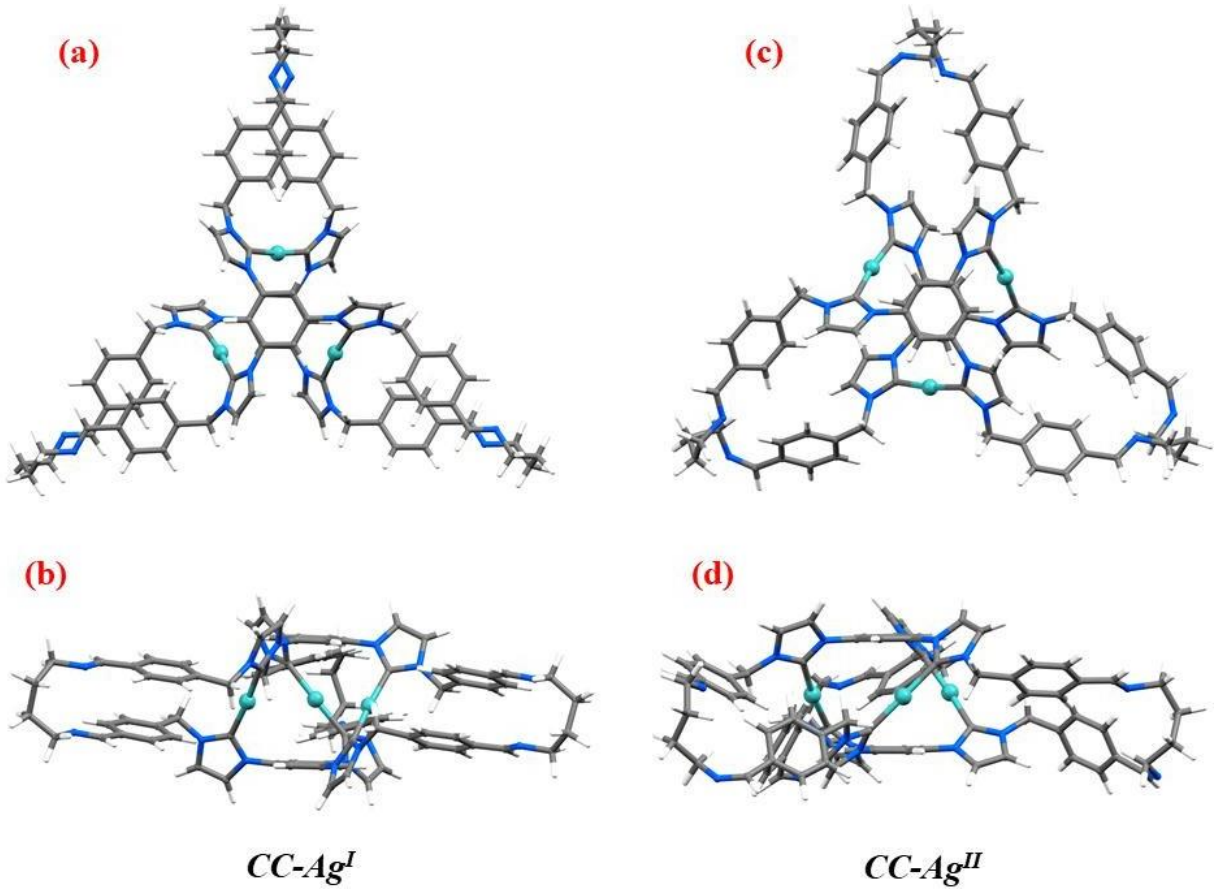

Fig. S29 DFT (B3LYP/6-31G) optimized structures of **CC-Ag^{I}** (a, b) and **CC-Ag^{II}** (c, d). [Top view and Side view]

References:

1. B. C. Bookser and T. C. Bruice, *J. Am. Chem. Soc.*, 1991, **113**, 4208-4218.
2. M. J. Frisch, G. W. Trucks, H. B. Schlegel, G. E. Scuseria, M. A. Robb, J. R. Cheeseman, G. Scalmani, V. Barone, B. Mennucci, G. A. Petersson, H. Nakatsuji, M. Caricato, X. Li, H. P. Hratchian, A. F. Izmaylov, J. Bloino, G. Zheng, J. L. Sonnenberg, M. Hada, M. Ehara, K. Toyota, R. Fukuda, J. Hasegawa, M. Ishida, T. Nakajima, Y. Honda, O. Kitao, H. Nakai, T. Vreven, J. A. Montgomery, J. E. Peralta, F. Ogliaro, M. Bearpark, J. J. Heyd, E. Brothers, K. N. Kudin, V. N. Staroverov, R. Kobayashi, J. Normand, K. Raghavachari, A. Rendell, J. C. Burant, S. S. Iyengar, J. Tomasi, M. Cossi, N. Rega, J. M. Millam, M. Klene, J. E. Knox, J. B. Cross, V. Bakken, C. Adamo, J. Jaramillo, R. Gomperts, R. E. Stratmann, O. Yazyev, A. J. Austin, R. Cammi, C. Pomelli, J. W. Ochterski, R. L. Martin, K. Morokuma, V. G. Zakrzewski, G. A. Voth, P. Salvador, J. J. Dannenberg, S. Dapprich, A. D. Daniels, Farkas, J. B. Foresman, J. V. Ortiz, J. Cioslowski and D. J. Fox, Wallingford CT, 2009.
3. S. Grimme, *J. Comput. Chem.*, 2006, **27**, 1787-1799.
4. S. Grimme, *J. Comput. Chem.*, 2004, **25**, 1463-1473.